Evidence for the Decay of Nuclear Matter Toroidal Geometries in Nucleus-Nucleus Collisions

N. T. B. Stone,[1,*] O. Bjarki,[1] E. E. Gualtieri,[1] S. A. Hannuschke,[1] R. Lacey,[2] J. Lauret,[2] W. J. Llope,[3] D. J. Magestro,[1] R. Pak,[1] A. M. Vander Molen,[1] G. D. Westfall,[1] and J. Yee[1]

[1]*National Superconducting Cyclotron Laboratory and Department of Physics and Astronomy, Michigan State University, East Lansing, Michigan 48824-1321*

[2]*Department of Chemistry, State University of New York at Stony Brook, Stony Brook, New York 11794-3400*

[3]*T. W. Bonner Nuclear Laboratory, Rice University, Houston, Texas 77251*

(Received 23 July 1996)

Systematic experimental evidence is presented for the decay of nuclear matter from toroidal geometries using reactions of ^{86}Kr + ^{93}Nb at incident energies ranging from 35 to 95 MeV/nucleon. The decay of noncompact geometries is established through two charge-related observables, and the distinction between toroidal and bubblelike geometries is achieved through event shape analysis. Indications of these exotic geometries appear for beam energies between 60 and 75 MeV/nucleon. [S0031-9007(97)02731-2]

PACS numbers: 25.70.Pq, 21.10.Gv

Recent theoretical calculations based on transport theories have predicted the occurrence of exotic breakup geometries at intermediate energies [1–6]. These geometries include bubbles and toroids, which are considered noncompact because of their hollow centers, as well as disks. Experimental searches to date have not been able to confirm these predictions [7–9]. In this Letter we present a study of central collisions in the ^{86}Kr + ^{93}Nb system at incident energies ranging from 35 to 95 MeV/nucleon. Our results comprise the first systematic experimental results which both provide evidence for the decay of nuclear matter from a toroidal geometry and confine this occurrence to a finite range of beam energies. We use two experimental observables, based on intermediate mass fragment multiplicities and charge similarity, to establish that the system decays from a noncompact breakup geometry. We then use event shape analyses to show that the decaying system is more consistent with a coplanar shape, thus implying that the geometry is toroidal. We find that the toroidal geometries are produced for beam energies between 60 and 75 MeV/nucleon.

The experimental data in this study were collected using the ^{86}Kr + ^{93}Nb system for the beam energies 35, 45, 50, 55, 60, 65, 75, 85, and 95 MeV/nucleon using the MSU 4π Array [10]. Immediately prior to this study, the Array was upgraded, extending the forward coverage for heavy fragments ($Z \lesssim 27$) down to 0.5° from the beam axis. Subarrays forward of 18° have lower energy thresholds of approximately 10 MeV/nucleon for ^{7}Li, and those between 18° and 162° have a corresponding threshold of 3 MeV/nucleon. Although these thresholds prohibit a detailed analysis of low-energy kinetic energy spectra, we present below a number of other available experimental signatures.

Our study includes only central events from this data set because the formation of noncompact geometries is predicted for central events [2,4]. We selected central events from our data by using the well-established method of imposing cuts on global observables called centrality variables [11,12]. In order to avoid autocorrelations between the centrality variables and the experimental signatures that we present, we have used two different centrality variables: the total transverse kinetic energy [$E_t = \sum_{i=1,N_c} E_i \sin^2(\theta_i)$], and the total charge of detected fragments traveling at midrapidity ($Z_{\rm mr} = \sum_{i,0.75y'_{targ}<y'_{frag,i}<0.75y'_{proj}} Z_i$) [12], where N_c is the number of detected charged particles, E_i is the kinetic energy of each fragment, and y'_{targ}, $y'_{frag,i}$, and y'_{proj} are the center-of-momentum frame rapidities of the target, emitted fragments, and projectile, respectively. To ensure the centrality of the data sample, we applied cuts on E_t accepting only the 5% most central events when dealing with charge-based signatures and similar 5% cuts on $Z_{\rm mr}$ when dealing with the event shape signatures. More stringent event selection (based on, e.g., fragment emission geometry or alignment) may enhance some predicted signatures at the expense of clarity and generality, but are not needed to establish the signatures shown below.

The first experimental signature we present is an anomalous increase in the number of intermediate-mass fragments (IMFs). An IMF is defined as a fragment with a charge in the range $3 \leq Z \lesssim 20$. Published percolation model calculations quantitatively demonstrate that decay from noncompact geometries (toroids and bubbles) will result in emission of more IMFs than would be otherwise observed in the decay of a compact spherical geometry [8]. We have measured the multiplicity of IMFs in central events selected via cuts on E_t and plotted the mean values versus the incident beam energy per nucleon in Fig. 1(a). Statistical error bars are smaller than the marker size. Two features are clear in Fig. 1(a). The first is a general trend in which this multiplicity increases with increasing beam energy. This trend in IMF emission has been documented in previous experimental studies

 0031-9007/97/78(11)/2084(4)$10.00

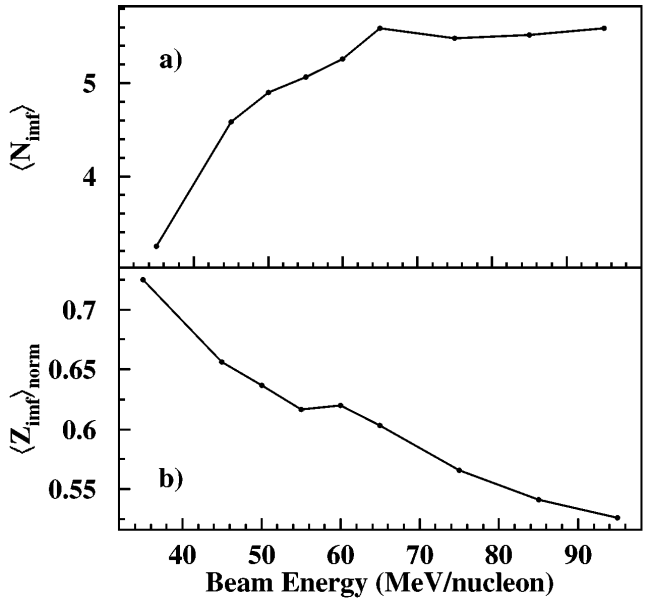

FIG. 1. (a) Mean intermediate-mass fragment multiplicity. (b) Total charge of IMFs normalized by the midrapidity charge, plotted versus the incident beam energy.

[13,14]. The second feature is an increase in the mean IMF multiplicity which deviates from the more basic trend at a beam energy of 65 MeV/nucleon. Examination of the N_{imf} distributions themselves reveals that this approximate 5% deviation in the mean value is due to a shift in the overall distribution, not to a change in its shape. This qualitative enhancement is consistent with the increase in IMF emission predicted to accompany the formation of noncompact geometries [2,4,8] over a limited energy range, and thus provides our first confirmation.

The enhancement in IMF emission shown in Fig. 1(a) can be further examined by plotting the total charge of detected IMFs divided by the total charge of particles traveling at midrapidity ($\langle Z_{\mathrm{imf}} \rangle_{\mathrm{norm}}$). Because the midrapidity charge roughly corresponds to the size of the emitting source, in this way we divide out the (changing) size of the source and obtain a normalization for the amount of the system emitted as IMFs. This quantity is plotted in Fig. 1(b), and shows an overall trend consistent with the decreasing prevalence of charge bound in IMFs. It also shows a 5% enhancement reminiscent of the IMF multiplicity enhancement shown in Fig. 1(a), although at a slightly lower energy. We shall return to this latter point at length. This enhancement is also due to a shift in the distributions and not to a change in their shape. Thus, we observe the enhancement signature in IMF emission even when factoring in the increasing size of the emitting system.

The second signature we present is an enhanced similarity in the charges of large fragments. Some theoretical models have quantitatively predicted that the formation of noncompact geometries will also result in increased cross sections for the emission of fragments with nearly equal masses [4,15]. To quantify this phenomenon for our data, we have calculated the power-law exponents for ordered Z distributions. This calculation begins with the ordering of the charges of the detected fragments, from largest to smallest, on an event-by-event basis. In this way, each fragment is assigned an index from 1 to N_c, the total number of charged particles. We then calculate the mean charge for each of these indexed charges over all events in our sample. We have observed empirically that these ordered Z distributions are best reproduced by a power law [i.e., $\langle Z_{\mathrm{ord}}(i) \rangle \propto i^{-\alpha}$], although the qualitative features of the signature we present below are insensitive to the fit type. It follows that the fit parameter α for these distributions would be small (large) for events which contain very similarly (differently) charged fragments. Thus, the presence of a noncompact breakup geometry giving rise to more similarly charged large fragments should be accompanied by a suppressed value of this exponent.

We have extracted the power-law exponent α for central events selected via cuts on E_t and plotted them versus the beam energy in Fig. 2(a) (solid lines). Statistical errors are smaller than the markers, and systematic fitting errors are plotted. We observe an overall trend in α, decreasing with increasing beam energy, corresponding to an increasing probability for the emission of IMFs having similar sizes. It is clear that this observable, like the IMF multiplicity, also undergoes a (5%) departure from the overall smooth trend, and at a similar beam energy.

The solid lines depict those values obtained by fitting only the three largest charges in each event. These are compared directly to another quantitative measure of charge symmetry ($\langle D_{\mathrm{cent}} \rangle$) obtained from Dalitz plots (Ref. [16]). D_{cent} is defined as the distance from the

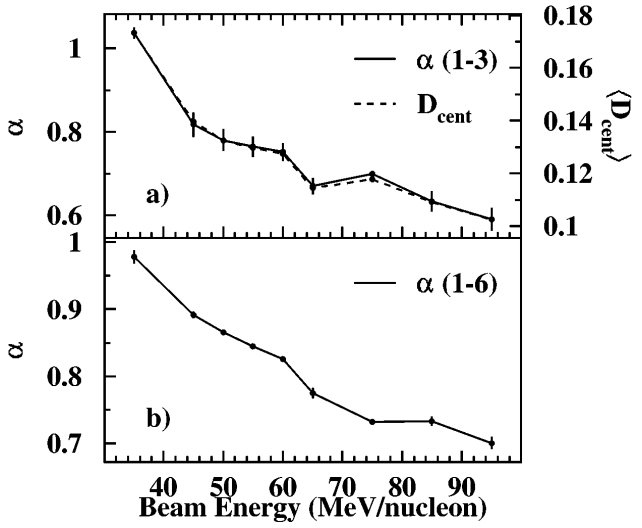

FIG. 2. (a) Extracted α values (solid line) and D_{cent} values (dashed line) both calculated using only the largest three fragments. (b) Extracted α values obtained using the largest six fragments, plotted versus the incident beam energy.

center of a Dalitz triangle to the coordinates calculated from the charges of the three largest fragments in each event, such that small (large) values of $D_{\rm cent}$ correspond to events having similar (dissimilar) charges. The comparison of the mean values of $D_{\rm cent}$ (dashed) to those obtained for α (solid) illustrates that our method of using ordered-charge distributions reproduces the results of other well-known charge similarity observables. However, the advantage to the latter method is that it can be applied to an arbitrary number of particles.

Because we have established [Fig. 1(a)] that $\langle N_{\rm imf}\rangle \sim 5.5$ for this system, we have extracted the exponent α by fitting the first six charges [Fig. 2(b)]. The reduction in systematic error resulting from the inclusion of a broader fit range is also evident from Fig. 2(b). In this case, the extracted α values at 65 and 75 MeV/nucleon are suppressed so that they lie below the values consistent with the overall smoothly decreasing trend. This suppression in α (and in $D_{\rm cent}$) is an indication of more equally sized large fragments and has been predicted to accompany the formation of noncompact geometries [4]. By comparing Fig. 2, frames (a) and (b), we show again that the precise energies of this phenomenon are slightly different, and depend somewhat on the details of the definition of the observables.

Based on these quantitative and qualitative predictions, the two charge-based observables shown above (multiplicity and similarity) demonstrate trends that are well explained by the decay of noncompact geometries. However, to differentiate between the possibilities of toroid and bubble formation an additional signature is required. The use of event shape observables to make precisely this distinction was proposed by the authors of Ref. [4].

The third signature we present is a suppressed sphericity in the emission of heavy fragments. It is derived from the sphericity of particle emission in momentum space, and it ascribes a quantitative measure to the dimensionality of the breakup geometry. Such an observable includes all of the information measured for each fragment (i.e., charge, energy, emission angles), and thus provides a good balance to observables based on charges alone. Sphericity is defined [17] by first generating the kinetic energy tensor such that $T_{ij} = \sum_{n=1}^{N_{\rm imf}} (p_{i,n} p_{j,n})/2m_n$, where $N_{\rm imf}$ is the number of IMFs in each event, and $p_{i,n}$ and m_n are the ith component of the momentum and the mass of each IMF, respectively. Next, the eigenvalues (λ_i) of this tensor are calculated, ordered ($\lambda_1 > \lambda_2 > \lambda_3$), and normalized ($q_i = \lambda_i / \sum_{j=1}^{3} \lambda_j$), and the sphericity is defined as $S = \frac{3}{2}(q_2 + q_3)$. Given this definition, events with isotropic emission of IMFs will have a high value of sphericity, while those with coplanar or otherwise nonspherical emission will have lower values. It is known that the range of allowed values of sphericity is affected by the multiplicity of particles ($N_{\rm imf}$) in the tensor sum. To account for this effect, we compare events having the same IMF multiplicities [18]. We will also extract from this tensor the flow angles [$\cos(\theta_i)$] which correspond to the alignment of each of the eigenvectors and are obtained directly via the dot product of the eigenvectors with the z axis. By the ordering of eigenvalues described above, θ_1 thus corresponds to the azimuthal angle of the eigenvector associated with the largest eigenvalue.

We have calculated the mean values of the sphericity of IMF emission ($\langle S\rangle$) for central events selected via cuts on $Z_{\rm mr}$ and plotted these (markers) versus the incident beam energy per nucleon for one representative IMF multiplicity ($N_{\rm imf} = 5$) in Fig. 3(a). The trends observed for other multiplicities are nearly identical to those shown. Statistical errors on the mean values are smaller than the marker size and systematic errors are shown. We have plotted above and below the values obtained from the experimental data the resulting mean values obtained from the output of an event generator [19] which produced spherical (dotted lines) and disklike (dot-dashed lines) emission patterns. The significant input parameters to this model were the aspect ratio of the ellipsoid of particle emission, the emission source temperature, and charge and multiplicity distributions. The aspect ratios used were 1:1:1 and 2.5:2.5:1 for the sphere and disk simulations, respectively, and source temperatures were extracted from relativistic Maxwell-Boltzmann fits to experimental energy spectra for $Z = 3$ (the smallest IMF) fragments. Charge and multiplicity distributions were constrained to match the observed experimental distributions resulting in central events. The output from this model was then filtered through a detailed software replica of our detector which accounted for effects such as upper and lower kinetic energy thresholds, uncovered solid angle, malfunctioning detectors, and multiple particle hits. Thus we can

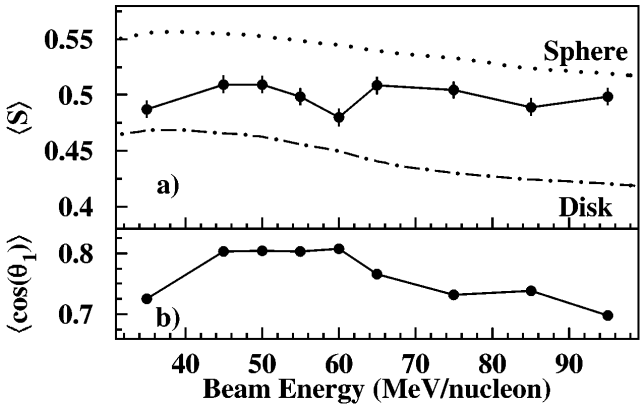

FIG. 3. (a) Measured values of the mean sphericity of IMF emission (markers) versus the incident beam energy. The dotted and dot-dashed lines indicate the mean values obtained for filtered spherical and disklike simulations, respectively. (b) Cosine of the flow angle corresponding to the largest eigenvalue, plotted versus the incident beam energy.

compare the sphericity values for these simulated emission patterns directly to our experimental data.

The sphericity values resulting from the disklike simulation are lower than those resulting from the spherical simulation. This difference illustrates the effectiveness of sphericity in quantitatively distinguishing disklike emission from spherical emission. Second, an examination of the excitation function of the sphericity values yielded by the filtered simulation reveals that changes in the acceptance effects on $\langle S \rangle$ with increasing beam energy are smooth, so that any significant change in the experimental data that does not follow this smooth trend cannot be attributed to systematic changes in acceptance.

The experimental values of sphericity fall between the limiting values obtained for the spherical and disklike simulations, and the shape of the curve reflects the same basic trends which we associate here with acceptance effects. However, at a beam energy of 60 MeV/nucleon, the experimental value of $\langle S \rangle$ is suppressed by 5%, approaching the disklike values. This suppression, reflecting a shift in the sphericity distributions, cannot be attributed to experimental acceptance and is beyond statistical fluctuations, indicating more disklike, or coplanar, IMF emission at this energy. The value of sphericity achieved at 60 MeV/nucleon is consistent with a disk of aspect ratio 2:2:1. Parallel analysis of other event shape observables (e.g., coplanarity) reveals corresponding suppression/enhancement signatures at the same beam energy. This trend shown in the event shape observables confirms the occurrence of a more two-dimensional breakup geometry.

In the case of toroid formation (Ref. [2]), the torus is oriented perpendicular to the beam axis. Thus a perfectly central collision would give rise to two comparatively large eigenvalues with eigenvectors perpendicular to the beam axis, so that the three signatures presented above would be further corroborated by a suppression in the cosine of the first flow angle [$\cos(\theta_1)$, as previously defined]. The mean value of this cosine is plotted in Fig. 3(b), and does show a suppression, although at a slightly different energy than that shown in Fig. 3(a). This transition to a more perpendicular orientation is the fourth independent signature we present as evidence for the decay of toroidal geometries.

The subtle and recurring variation in the energy of toroidal breakup as presented in this Letter suggests a variation in the sensitivities of specific observables, dependent upon their definitions. These differences prohibit the precise location of a transitional beam energy and merits further inquiry. However, all observables exhibit sensitivity to the occurrence of this phenomenon and together form strong experimental support for the formation of toroidal geometries.

We have presented a systematic study of four independent global experimental observables for the ^{86}Kr + ^{93}Nb system for incident energies ranging from 35 to 95 MeV/nucleon. Our study reveals a 5% enhancement in emission of intermediate-mass fragments and in similarity in the charges of these large fragments, which together establish the noncompact nature of the breakup geometry. We also observe a 5% suppression in the mean value of the sphericity and suppressed flow angles of IMF emission, which indicate toroidal, as opposed to bubblelike, geometries. All of these signatures occur at energies between 60 and 75 MeV/nucleon. These signatures are predicted by many of the same theoretical models that have provided us with the most recent descriptions of noncompact geometries, and should be interpreted in that context as experimental evidence for the existence of toroidal breakup geometries.

We gratefully acknowledge the assistance of J. Svoboda in the data reduction. This work was supported by the NSF under Grants No. PHY-92-14992 and No. PHY-95-28844 (NSCL/MSU).

*Current address: Ernest Orlando Lawrence Berkeley National Laboratory, Berkeley, CA 94720.

[1] L. G. Moretto *et al.*, Phys. Rev. Lett. **69**, 1884 (1992).
[2] W. Bauer, G. F. Bertsch, and H. Schulz, Phys. Rev. Lett. **69**, 1888 (1992).
[3] D. H. E. Gross, B. A. Li, and A. R. DeAngelis, Ann. Phys. (Leipzig) **1**, 467 (1992).
[4] H. M. Xu *et al.*, Phys. Rev. C **48**, 933 (1993).
[5] S. R. Souza and C. Ngô, Phys. Rev. C **48**, R2555 (1993).
[6] A. Guarnera *et al.*, GANIL Report No. P95-05, 1995.
[7] T. Glasmacher, C. K. Gelbke, and S. Pratt, Phys. Lett. B **314**, 265 (1993).
[8] L. Phair, W. Bauer, and C. K. Gelbke, Phys. Lett. B **314**, 271 (1993).
[9] L. G. Moretto, K. Tso, and G. J. Wozniak, Phys. Rev. Lett. **78**, 824 (1997).
[10] G. D. Westfall *et al.*, Nucl. Instrum. Methods Phys. Res., Sect. A **238**, 347 (1985).
[11] C. Cavata *et al.*, Phys. Rev. C **42**, 1760 (1990).
[12] L. Phair *et al.*, Nucl. Phys. **A548**, 489 (1992).
[13] G. F. Peaslee *et al.*, Phys. Rev. C **49**, R2271 (1994).
[14] W. J. Llope *et al.*, Phys. Rev. C **51**, 1325 (1995).
[15] C. Y. Wong, Ann. Phys. (N.Y.) **77**, 279 (1973).
[16] N. T. B. Stone *et al.*, Phys. Rev. C **51**, 3157 (1995), and references therein.
[17] G. Fái and J. Randrup, Nucl. Phys. **A404**, 551 (1983).
[18] W. J. Llope *et al.*, Phys. Rev. C **52**, 1900 (1995).
[19] E. E. Gualtieri, Ph.D. dissertation, Michigan State University, 1995 (unpublished).
[20] J. Cugnon and D. L'Hote, Nucl. Phys. **A397**, 519 (1983).